A genetic and physical study of the interdomain linker of *E. Coli* AraC protein-a *trans*-subunit communication pathway

Fabiana Malaga,[1] Ory Mayberry,[2] David J. Park,[3] Michael E. Rodgers,[2] Dmitri Toptygin,[2] and Robert F. Schleif[2]*

[1] Biology Department, UPCH, Lima, San Martín De Porres, Peru

[2] Department of Biology, Johns Hopkins University, Baltimore, Maryland 21218

[3] Tufts University Medical School, Boston, Massachusetts

ABSTRACT

Genetic experiments with full length AraC and biophysical experiments with its dimerization domain plus linker suggest that arabinose binding to the dimerization domain changes the properties of the inter-domain linker which connects the dimerization domain to the DNA binding domain via interactions that do not depend on the DNA binding domain. Normal AraC function was found to tolerate considerable linker sequence alteration excepting proline substitutions. The proline substitutions partially activate transcription even in the absence of arabinose and hint that a structural shift between helix and coil may be involved. To permit fluorescence anisotropy measurements that could detect arabinose-dependent dynamic differences in the linkers, IAEDANS was conjugated to a cysteine residue substituted at the end of the linker of dimerization domain. Arabinose, but not other sugars, decreased the steady-state anisotropy, indicating either an increase in mobility and/or an increase in the fluorescence lifetime of the IAEDANS. Time-resolved fluorescence measurements showed that the arabinose-induced anisotropy decrease did not result from an increase in the excited-state lifetime. Hence arabinose-induced decreases in anisotropy appear to result from increased tumbling of the fluorophore. Arabinose did not decrease the anisotropy in mutants incapable of binding arabinose nor did it alter the anisotropy when IAEDANS was conjugated elsewhere in the dimerization domain. Experiments with heterodimers of the dimerization domain showed that the binding of arabinose to one subunit of the dimer decreases the fluorescence anisotropy of only a fluorophore on the linker of the other subunit.

INTRODUCTION

The *Escherichia coli* regulatory protein, AraC, is a member of a very large class of prokaryotic regulatory proteins.[1] Except for AraC protein, which has been intensively studied for >40 years, surprisingly little biochemical information is available on the other family members except for those like SoxS[2] and MarA[3] which are monomeric and consist of only a DNA binding domain. The paucity of biochemical information on the "full length," two-domain, dimeric, AraC family members such as XylS, MelR, RhaR, RhaS, and ToxT[1,4] is a consequence of the fact that these proteins are at best sparingly soluble and sometimes cannot be purified at all. With considerable effort it has proven possible to purify and study at low concentrations a few AraC

mutants.[5] The two domains of AraC, the dimerization domain[6] and the DNA binding domain[7] themselves are fairly well behaved, however, and each can be purified and studied.

In the absence of arabinose, AraC protein, the dimeric regulator of the L-arabinose operon in *E. coli*, actively represses expression of the promoter for the *araB*, *araA*, and *araD* genes, p_{BAD},[8–10] by forming a DNA loop between the I_1 half-site at p_{BAD} and the O_2 half-site located 210 base pairs away.[10–13]
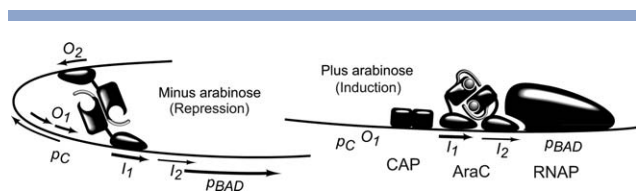
Figure 1

Structure of the arabinose operon regulatory region.

Upon the binding of arabinose most of the protein shifts and instead, binds to the adjacent direct repeat DNA half-sites I_1 and I_2, (Fig. 1)[10,14] where it actively stimulates transcription.[8,15–17] Arabinose does not appear to shift the relative affinities in binding to the similar, but nonidentical DNA half-sites involved. Instead, *in vivo* and *in vitro* binding data indicate that in the presence of arabinose, the DNA binding domains of AraC are more free to adopt the positions and relative orientations required for binding to direct repeat sites than in the absence of arabinose.[14,18]

The 20-residue N-terminal arms of AraC play an important role in coupling arabinose binding in the dimerization domain to the protein's DNA binding and DNA looping properties. Partial deletions or almost any point mutation in the arm cause the protein to lose part or all of its ability to repress by looping, but not its ability to induce. Such mutant proteins are said to be constitutive because, even in the absence of arabinose, they bind to I_1 and I_2 and induce transcription from p_{BAD}.[19,20] Also, crystal structures of dimerization domain indicate that in the presence of arabinose, but probably not in its absence, the N-terminal arms of full length AraC bind directly over the arabinose-binding pockets of the dimerization domain.[6,21]

Collectively, these results suggest that in the absence of bound arabinose, the N-terminal arms function to position and orient the DNA binding domains such that binding to O_2 and I_1 is energetically favored. When arabinose binds, the DNA binding domains become less constrained, likely in conjunction with repositioning of the arms. This changes the energetics such that binding to I_1 and I_2 is now favored. Consequently, the increased occupancy of I_1 and I_2 increases transcription initiating at p_{BAD}.

A simple molecular mechanism consistent with the aforementioned facts would be for the N-terminal arms to bind directly to nearby DNA, to the DNA binding domains, or to both, in the absence of arabinose to aid in restraining the positions adopted by the DNA binding domains. A priori, the simplest possibility seems to be direct binding of the N-terminal arms of AraC to the protein's C-terminal DNA binding domains. A number of experiments have failed, however, to provide definitive

evidence for such an interaction. These include genetics approaches,[22,23] and physical approaches including surface plasmon resonance,[24] NMR,[25] and fluorescence anisotropy.[25]

In light of the failures to detect an arm-DBD interaction we have extended consideration to the possibility that the binding of arabinose, either directly via the N-terminal arms or indirectly, affects the inter-domain linker, residues 168–174, that connects each dimerization domain and a DNA binding domain. Although initial genetics experiments suggested that the repressing and inducing activities of AraC are not sensitive to sequence alterations in the linker,[26] more recent and more precisely targeted mutational and biophysical studies have indicated that some mutations in the linker can reduce the protein's ability to repress p_{BAD}.[27] This article describes an expanded genetic analysis of linker mutations and fluorescence anisotropy measurements that show that binding of arabinose to the dimerization domain alters the motion of a conjugated fluorophore. The findings are compatible with arabinose altering the apparent flexibility of the inter-domain linker with control likely being exerted on the linker itself. It is possible, but far from demonstrated that this forms the basis for the arabinose-induced change in the DNA looping properties of AraC. In the ideal case, the fluorescence anisotropy measurements, which can measure molecular tumbling, would be performed on full length AraC with the fluorophore attached to the DNA binding domain. Such experiments, however, are currently not feasible in part due to the limited solubility of AraC. Consequently, the anisotropy experiments were performed only on dimerization domain plus linker without the DNA binding domain.

MATERIALS AND METHODS

Mutant isolation and characterization

The *araCp_{BAD}*-GFP plasmid is derived from pBR322 plasmid,[28] and carries the *araC* gene, the regulatory region between *araC* and *araB* and the sequence specifying the first 15 nucleotides of the transcript from the *ara p_{BAD}* promoter. Beyond the initial *ara* transcribed sequence are 42 nucleotides of upstream sequence of the GFP gene, and then the gene itself. This plasmid was briefly sold by Clontech. It places expression of green fluorescent protein under control of the *ara p_{BAD}* promoter and was used in the present experiments for the isolation and characterization of linker mutants. The entire plasmid was mutagenized by passing the plasmid through the mutator strain XL1-Red (*endA*1 *gyrA*96 *thi*−1 *hsdR*17 *supE*44 *relA*1 *lacmutD*5 *mutS mutT* (Stratagene). For a higher level of mutagenesis and for direction of mutations to just the *araC* gene, the coding region of the *araC* gene was amplified by error-prone PCR mutagenesis and placed in the *araCp_{BAD}*-GFP plasmid following

the GeneMorph II EZClone domain mutagenesis procedure (Stratagene). Finally, for the introduction of specific mutations and for the randomization of sets of one, two, or three codons in the linker region of *araC* we used the Stratagene QuikChange protocol for oligonucleotide directed mutagenesis. Mutagenized plasmids were transformed into strain SH321(Δ*araC-leu1022* Δ*lac74 galK thi1*),[29] and plated on tryptone-yeast extract medium[30] so that repression negative mutants could be identified by colony fluorescence. To identify any arabinose negative mutants, isolated fluorescent and nonfluorescent colonies were spotted on minimal glycerol and minimal arabinose solid media. Candidates were grown in liquid medium both for sequencing of their plasmid DNA and for assay of arabinose isomerase.

Arabinose isomerase levels were measured in cells growing in M10 minimal salts medium containing 1% casamino acids, 0.2% glycerol, and plus or minus 0.2% arabinose as described.[30]

Purification and labeling of dimerization domain plus linker

All the *in vitro* experiments were performed with dimerization domain containing the Y31V mutation. This mutation substantially reduces aggregation tendencies of the domain.[21] The various mutant dimerization domain proteins, residues 1–182 of AraC plus a C-terminal hexahistidine tag, were overproduced using the pET21 vector (Novagene), isolated using immobilized metal ion affinity chromatography, subjected to light trypsin digestion to cleave specifically at R178, and separated from residues 179–182 and the His$_6$ tag by chromatography on HiTrap-Q HP columns as described.[21]

To label, the protein was reduced with a 10-fold excess of TCEP, (tris(2-carboxyethyl)phosphine) before addition of a 20-fold molar excess of IAEDANS (Invitrogen) dissolved in one quarter of the solution's volume in DMSO. This was allowed to react overnight at room temperature. A two fold molar excess of β-mercaptoethanol over the IAEDANS was added and the solution was diluted three fold with 15 mM Tris-Cl, pH 8.0, 5 mM L-arabinose and 10 mM NaCl and purified by passage over the HiTrap-Q HP column as above. Typically, three partially overlapping protein peaks eluted from the column in the order of unlabeled, singly labeled, and doubly labeled protein. The amounts of the three species indicated that the labeling efficiency varied between 50 and 100%. Labeled dimerization domain was further separated from residual free dye and arabinose by dialysis against 15 mM Tris-Cl pH 8, 50 mM NaCl for 3 × 24 h.

Mass spectrometry of labeled dimerization domain

Twenty-five micrograms of dimerization domain in 50 μL was mixed with 20 μL 500 mM (NH$_4$)HCO$_3$, 6.5 μL H$_2$0, and 4.5 μL 100 mM DTT, heated to 95°C for 5 min. Then 9 μL 100 mM iodoacetamide was added and incubated 30 min in the dark before quenching alkylation with the addition of 2.5 μL of 100 mM DTT. The sample was desalted by passage through a PrepClean C-18 Spin Column (Pierce), dried and resuspended in aqueous 5% (v/v) acetonitrile, 0.1% formic acid. For proteolytic cleavage, 2.5 μL MS grade trypsin (Pierce) at 0.2 mg/mL was added to the alkylated sample for digestion at 37° C for 24 h. After digestion, the samples were desalted with the C-18 spin column.

Electrospray mass spectrometry was performed on a Waters Acquity-Xevo G2 (UPLC-MS/MS). Intact proteins were chromatographed on a C-4 column and eluted with a 10 min, 5–80% acetonitrile gradient at a flow rate of 0.3 mL/min. The eluate was passed through a UV/Vis diode array for detection of IAEDANS-labeled peptides prior to injection into the electrospray port of the mass spectrometer. Peptide samples were chromatographed on a C-18 column and eluted with a 12 min 5–80% acetonitrile gradient. Analysis of the data was performed using Mass Lynx software supplied by the vendor.

Fluorescence binding and steady-state anisotropy measurements

Measurements were performed on a T-format Photon Technology International fluorimeter equipped with a 75 watt xenon light source and a temperature controlled cuvette holder. Samples were continuously stirred in a 1 cm path length cuvette at 0.25–2.5 μM protein in 15 mM Tris-Cl pH 8.0, 50 mM NaCl, 1 mM DTT, and 1 mM EDTA in a final volume of 2.5 mL. In the heterodimer experiments, 100 mM NaCl or 100 mM KCl was substituted for the 50 mM NaCl, but these changes were without observable effect. Occasional early experiments were plagued by a background of steadily increasing anisotropy. As the vertically polarized light component was observed to be increasing anomalously in these cases, we attribute the increase to aggregation. The following steps largely eliminated the problem. Care was taken to choose column fractions of labeled protein containing a maximum of doubly labeled dimerization domain and a minimum of singly labeled protein, TCEP was added to the sample to a concentration of 0.2 mM, the nonionic detergent P20 was added to 0.01%, and the sample was subjected to centrifugation of 10,000g for 5 min immediately before a measurement.

Arabinose binding was quantitated by the change in average emission wavelength of the intrinsic tryptophan fluorescence of the AraC dimerization domain as a function of added arabinose. Samples were excited at 295 nm, the emission spectrum from 315 to 375 nm was recorded at a scan rate of 1 nm/s, and the entrance and exit slits were set for a spectral band width of 5 nm. After each arabinose addition, the solution was allowed

to equilibrate for 2 min before the next scan. An average emission wavelength at each titration point was calculated as:

$$\langle\lambda\rangle_{\text{em}} = \frac{\sum_{i=1}^{n}(I_i \times \lambda_i)}{\sum_{i=1}^{n}(I_i)}$$

where I_i is the fluorescence emission minus the background at the ith wavelength.[21] This was plotted against arabinose concentration and KaleidaGraph was used to determine λ_{offset}, λ_{em}, and K_{d} in the following equation.

$$\langle\lambda\rangle_{\text{em}} = \lambda_{\text{offset}} + \Delta\langle\lambda\rangle_{\text{em}} \times \left(\frac{[\text{L}-\text{arabinose}]}{K_{\text{d}} + [\text{L}-\text{arabinose}]}\right)$$

For the fluorescence anisotropy measurements the excitation and emission wavelengths were set to the peaks in the absorption and emission spectra of IAE-DANS, 336 nm and 490 nm, respectively. Monochromator slits were set to for a spectral band width of 10 nm. Fluorescence anisotropy (r) was calculated as:

$$r = \frac{I_{\|} - g \times I_{\perp}}{I_{\|} + 2 \times g \times I_{\perp}}$$

where $I_{\|}$ and $I_{\perp}$ are the fluorescence intensities of the parallel ($\|$) and perpendicularly ($\perp$) polarized emission when the sample is excited with vertically polarized light, and g is $I_{\|}/I_{\perp}$ for horizontally polarized excitation. The average anisotropy value over an 80-s interval for each titration point was calculated and plotted against arabinose concentration. To minimize the effects of statistical counting errors on the calculated values of anisotropy, sample concentrations were adjusted to yield between 100,000 and 1,000,000 counts per second. Minute-to-minute fluctuations in anisotropy, typically on the order of 0.001, can be attributed almost fully to statistical fluctuations in counting, but the day-to-day variations in the anisotropy of the same sample are on the order of 0.01 and seem to derive from a combination of sample and instrumental variation.

Time-resolved fluorescence measurements and data analysis

Time-resolved single-photon counting (TCSPC) data were obtained with a high-count-rate instrument built in the laboratory.[31] Fluorescence was excited with vertically-polarized picosecond laser pulses at 311 nm wavelength. Fluorescence emission was collected at 480 nm in T-format, through vertical and a horizontal polarizers. To minimize the effects of the differences between the two emission wings, each wing counted vertical emission photons 42% of the time, horizontal emission photons 42% of the time, and scattered excitation

photons 16% of the time. During one data acquisition the instrument switched 144 times between the three kinds of measurements. While the left wing counted vertical emission photons, the right wing counted horizontal emission photons, and vice versa, which minimized the effects of exciting intensity fluctuations. The vertical emission data from both wings were combined together as described,[31] and so were the horizontal emission data. This acquisition protocol together with two quartz-wedge achromatic depolarizers DPU-15 (one in each wing) ensured that the instrument had exactly equal sensitivity to both polarizations. To facilitate subsequent analysis, the TCSPC data for both polarizations were fitted simultaneously by the four equations for vertically and horizontally polarized intensity, $I_{\text{v}}(t)$ $I_{\text{h}}(t)$ and total intensity $I_{\text{total}}(t)$ and anisotropy $r(t)$.

$$I_{\text{v}}(t) = g^{+1/2}[1 + 2r(t)]I_{\text{total}}(t)$$

$$I_{\text{h}}(t) = g^{-1/2}[1 - r(t)]I_{\text{total}}(t)$$

$$I_{\text{total}}(t) = \sum_{n=1}^{N\text{int}} \alpha_n \exp(-t/\tau_n)$$

$$r(t) = \sum_{m=1}^{N\text{ani}} \beta_m \exp(-t/\varphi_m)$$

Similar equations except for the g factor that accounts for the difference in a real instrument's sensitivity to vertical and horizontal polarization can be found in Chapter 11 of the textbook written by Lakowicz.[32] Equations including the g factor were used in recent publications.[33–35] The g factor was calculated as the ratio of the live times for the vertical and horizontal emission data, respectively, and fixed during the model fitting. The live time of a multichannel analyzer represents the difference between the real time and the dead time.[31] Since the rate at which photons are counted is slightly higher for the vertical polarization, the live time is higher for the horizontal polarization, making the g factor slightly less than one (typically, about 0.97).

The horizontal and vertical intensity functions were numerically convoluted with the experimentally measured impulse response function and fit to the data using the method of least squares. The values of the parameters α_n, τ_n, β_m, and ϕ_m were adjusted during the fitting to minimize the χ^2. In addition to the best values of these fitting parameters, the method of least squares also produces the variance-covariance matrix.[36] The diagonal elements of this matrix equal squared standard deviations for the corresponding fitting parameters,[36] which was used to calculate the standard deviations reported in Table II.

The mean intensity weighted excited-state lifetime τ_{mean} and steady-state anisotropy r_{ss} values can be calculated from the time-resolved data as follows:

$$\tau_{\text{mean}} \equiv \frac{\displaystyle\int_0^\infty t I_{\text{total}}(t)\,\mathrm{d}t}{\displaystyle\int_0^\infty I_{\text{total}}(t)\,\mathrm{d}t} = \frac{\displaystyle\sum_n \alpha_n \tau_n^2}{\displaystyle\sum_n \alpha_n \tau_n}$$

$$r_{\text{ss}} \equiv \frac{\displaystyle\int_0^\infty r(t) I(t)_{\text{total}}\,\mathrm{d}t}{\displaystyle\int_0^\infty I_{\text{total}}(t)\,\mathrm{d}t} = \frac{\displaystyle\sum_n \sum_m \alpha_n \beta_m \left(\frac{1}{\tau_n} + \frac{1}{\varphi_m}\right)^{-1}}{\displaystyle\sum_n \alpha_n \tau_n}$$

The standard deviations for τ_{mean} or r_{ss} or any other function f of the fitting parameters can be expressed in terms of the variance-covariance matrix[36] where p_i are the elements of one array that contains all these fitting parameters α_n, τ_n, β_m, and ϕ_m, and C_{ij} are the elements of the variance-covariance matrix.

$$\sigma f = \sqrt{\sum_i \sum_j C_{ij} \left(\frac{\partial f}{\partial p_i}\right) \left(\frac{\partial f}{\partial pj}\right)}$$

RESULTS

Linker mutations—repression abilities

Previous searches for repression negative mutants sought high level constitutive phenotypes and primarily utilized the competitive inhibitor of L-arabinose induction, D-fucose.[19,22] These searches identified mutations that were largely confined to the N-terminal arm and to the base of the arm. To increase detection sensitivity so that rarer, lower level constitutive phenotypes, could be identified visually, we used a plasmid carrying both the *araC* gene and green fluorescent protein, GFP, whose expression is under control of the *ara* p_{BAD} promoter. Plasmid DNA was mutagenized by passage through a mutator strain, by error prone PCR amplification of the *araC* gene, or by oligonucleotide directed mutagenesis, then transformed into an *araC* deletion cell line and plated. Mutagenesis of the entire plasmid yielded approximately 0.5% fluorescent green colonies of widely variant fluorescence, and mutagenesis directed to just the *araC* gene yielded approximately 5% fluorescent green colonies.

Plasmids from a few of the intensely fluorescent green colonies obtained from mutagenesis of the plasmid or gene were sequenced and found to carry the previously isolated high level *araC* constitutive mutations, P11L, V20M, A152C, and A152V.[19,22] Amongst the lower level constitutive mutants were two previously known low level constitutives, L19Q, and R38L, and a new constitutive, N252D, at a position where other low level constitutives had previously been isolated. Also, the low level constitutives G12R, S14L, G22A, and G22D, were found

at positions where previously, only high level constitutives had been identified.

The new and interesting mutants resulting from the search are low level constitutives in positions at which no constitutives had previously been found, D33V, D37V, L156V, A166G, and H172P. Two of these, A166G and H172P lie in the inter-domain linker region. The distribution of the low level constitutives suggests that the eight-residue inter-domain linker region is a significant target for low level constitutives.

To explore the linker region more carefully, we randomized residues 167–172 of the linker region in sets of one, two, or three residues at a time. Table I displays the sequences of the variants with wild type phenotype and the sequences of repression impaired variants. The results are striking in that nearly any substitution lacking proline behaves as wild type, and nearly any substitution in the linker containing proline is impaired in its repression abilities. Because of this and an earlier finding that introduction of a proline residue into the linker region resulted in impaired repression,[27] we also explicitly generated proline substitutions in each of the linker residues 168–172, Table I. Repression in each of these was also impaired.

Fluorophore labeling of the inter-domain linker

In shifting from the repressing to the inducing state, the DNA binding domains significantly reposition, and as a result, the structure or conformation of the interdomain linkers must also change. Mutations in the linker, as observed in the previous section might, therefore, affect induction or repression. Are changes in linker structure accompanying changes in induction-repression the result of control exerted directly on DNA or the DNA binding domains, or are they a result of control exerted directly on the linkers? These two possibilities may be distinguishable by monitoring for structure changes in the linker, or lack thereof, in the absence of DNA and absence of the DNA binding domains.

Although NMR would seem to be suitable for determining the structure and dynamics of the linker in the presence and absence of arabinose, the relatively large size of the dimerization domain and the expense of this approach diminish its attractiveness. Instead of NMR, we chose to monitor properties of the linker in AraC in the absence of the DNA binding domains via fluorescence anisotropy of IAEDANS conjugated near the end of the linker. For this we introduced cysteine in place of residue M175 of the dimerization domain. After a typical conjugation reaction we found via mass spectrometry of intact dimerization domain that the labeling efficiency was about 60%, and after trypsin digestion, labeling of only the peptide containing M175C, with <1% labeling on any other peptide.
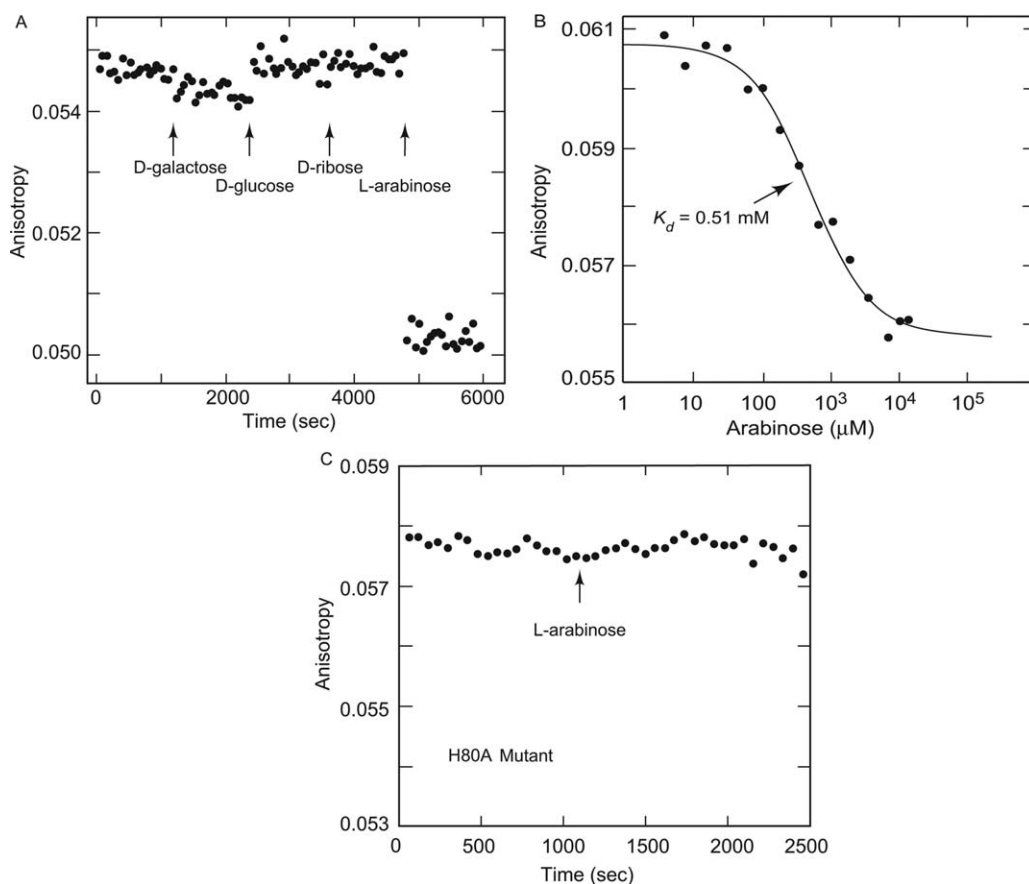
Table I
Linker Position, WT and Mutant Sequences

Repression plus (WT) linkers								Repression minus linkers							
167[a]	169		171			173		167	169		171			173	
I[b]	N	E	S	L	H	P	P	I	N	E	S	L	H	P	P
L	R	G							P[c,d]						
W	R	Q								P					
L	R	H									P				
G	S	F										P			
R	S	I											P		
T	H	H													
R	A	Q						K	K	E					
V	Y	R						C	P	C					
G	Q	Y						I	F	G					
Q	R	L						L	P	K					
G	L	F						R	P	R					
		L	I	E					M		S	N			
		A	R	R	S				G		P	R	P		
			N	L	L						D	M	P		
			A	S	K						C	S	P		
			Y	V	S						S	P	L		
			Y	D	N						K	P	P		
			W	R	R						K	K	A		
			L	S	Y						L	R	A		
			N	T	K	S					F	D	A		
			K	A	Q	I					F	K	Q		
			T	R	N	R					P	R	G		
			L	V	I	S					H	L	Y		
				L	R		E				G	A			
				V	A		F				P	N		L	
				L	L		S								
							A								
							A								
						R	A								
						A	G								
						T	L								
						L									

[a] Residue number.
[b] WT residue identity.
[c] All proline residues are highlighted.
[d] The uninduced, induced arabinose isomerase levels in units per cell, and colony fluorescence, respectively, of the proline substitution plasmids in SH321: WT, 14, 870, none; N168P, 210, 1500, green; E169P, 120, 1200, faint green; S170P, 51, 1500, very faint green; L171P, 110, 1400, faint green; H172P, 130, 1800, green. For the others, the repression plus mutants form white colonies and in the absence of arabinose contain less than 50 units isomerase per cell, and the repression minus mutants in the absence of arabinose formed faint to dark green fluorescent colonies and contained from 150 to 600 units per cell. All the mutants were inducible to between 800 and 2000 units isomerase per cell.

Arabinose-specific decrease in fluorescence anisotropy

Figure 2(A) shows the anisotropy of IAEDANS-labeled dimerization domain following the addition at the indicated times of D-galactose, D-glucose, D-ribose, and L-arabinose. Galactose and ribose addition produced no change in anisotropy while glucose addition induced a small increase of about 1% whereas arabinose addition generated a significant change, a reduction in the anisotropy of about 10%, from 0.06 to 0.054. Experiments in which the response was measured with only one sugar present at a time similarly showed that D-galactose, D-glucose, and D-ribose did not generate a significant change in anisotropy, (data not shown). Single addition experiments were also done with D-rhamnose, D-xylose, D-mannose, and D-fucose (an analog of L-arabinose). Of these sugars, only D-fucose produced a change in anisotropy, a reduction of about 2%, from 0.06 to 0.059 (data not shown). Anisotropy as a function of the arabinose concentration, [Fig. 2(B)] displays a simple ligand binding curve with a K_d of 0.51 mM, very close to the previously measured binding affinity of arabinose.[21,37] Nonetheless, as a further test that the arabinose-induced anisotropy decrease results from arabinose binding in the

Figure 2

Fluorescence anisotropy of IAEDANS conjugated to C175 of the dimerization domain plus linker of dimerization domain Y31V. (**A**) Sugars as indicated were added to a concentration of 40 mM. (**B**) Arabinose titration. (**C**) Arabinose addition to dimerization domain containing the H80A mutation.

sugar-binding pocket of the dimerization domain, we introduced the mutation H80A. This change in the arabinose-binding pocket prevents arabinose binding,[5] and in the present experiments [Fig. 2(C)], as expected, we found that the anisotropy of labeled H80A mutant dimerization domain does not change in response to arabinose addition.

Arabinose effect is limited to the inter-domain linker

On the basis of the data presented above, it is possible that the arabinose-induced decrease in the fluorescence anisotropy of the IAEDANS reflects an increased tumbling frequency of the protein as a whole. It is also possible, however, that the anisotropy decrease is a consequence of an increased fluorescence lifetime of the IAEDANS or is a consequence of a combination of the two. First we address the issue of tumbling as a whole, and in the next section, the issue of an increased excited-state lifetime.

If arabinose binding affects tumbling of the protein as a whole, then dimerization domain labeled at a position other than the linker should also display the arabinose-induced decrease in anisotropy. Residue E63 was chosen for alteration to cysteine and labeling because the side-chain of E63 is solvent exposed, lies in a β-sheet of the dimerization domain, and this location is remote from both the N-terminal arm and the linker. Thus, labeling at this position seems unlikely to interfere with function and no arabinose-induced environmental changes should occur to alter the fluorescence of the label.

Measurements of full length AraC containing the E63C mutation showed the protein to induce and repress very similar to wild type AraC. Addition of arabinose to the IAEDANS-labeled E63C dimerization domain indeed did not display the arabinose-induced decrease in anisotropy that is seen when the linker is labeled. Instead, the measurement reproducibly shows a small increase about one sixth of the magnitude of the decrease generated when the IAEDANS is conjugated to the end of the linker
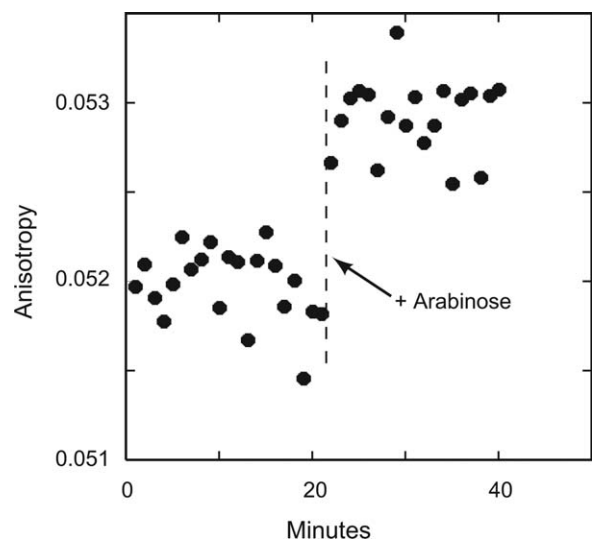
Figure 3

Anisotropy of E63C-IAEDANS dimerization domain. At 20 min. L-arabinose was added to a concentration of 40 mM.

(Fig. 3). We note in passing that the NMR ^{1}H-^{15}N HSQC spectrum of dimerization domain shows more and sharper resonances upon arabinose addition.[25] This and the anisotropy result are consistent with the domain's fluctuating between two or more conformational states in the absence of arabinose and being more biased toward one conformational state once arabinose is bound.

Arabinose does not lengthen the excited-state lifetime of linker-bound IAEDANS

To examine the contributions of changes in tumbling and changes in excited-state lifetime to the arabinose-induced decrease in steady-state anisotropy we performed TCSPC measurements of the labeled protein in the presence and absence of arabinose. This was done with polarizer settings that allowed extraction of both time-resolved intensity and time-resolved anisotropy. Although only the excited-state lifetimes were required from these experiments for interpretation of the steady-state data, the predicted steady-state anisotropy values could also be calculated from the time-resolved intensity and anisotropy data.

Figure 4 shows the plus and minus arabinose time-resolved horizontal and vertical fluorescence polarization data and the weighted residuals after multi-exponential fits to the data. The data presented in Figure 4 contain 60 million photon counts for the vertical polarization and 50 million photon counts for the horizontal polarization, which was made possible by the use of high (4 MHz) excitation pulse rate and two identical fluorescence emission wings in parallel.[31] Over fifty million photon counts per decay curve combined with 65 ps time resolution (full width at half maximum) made it possible to resolve four exponential terms in the intensity and anisotropy data. The data and fits with the plus arabinose sample are highly similar to those in Figure 4 and are not shown. Table II shows the parameter values that resulted in the best fits, both in the absence and presence of arabinose. These values of the parameters give
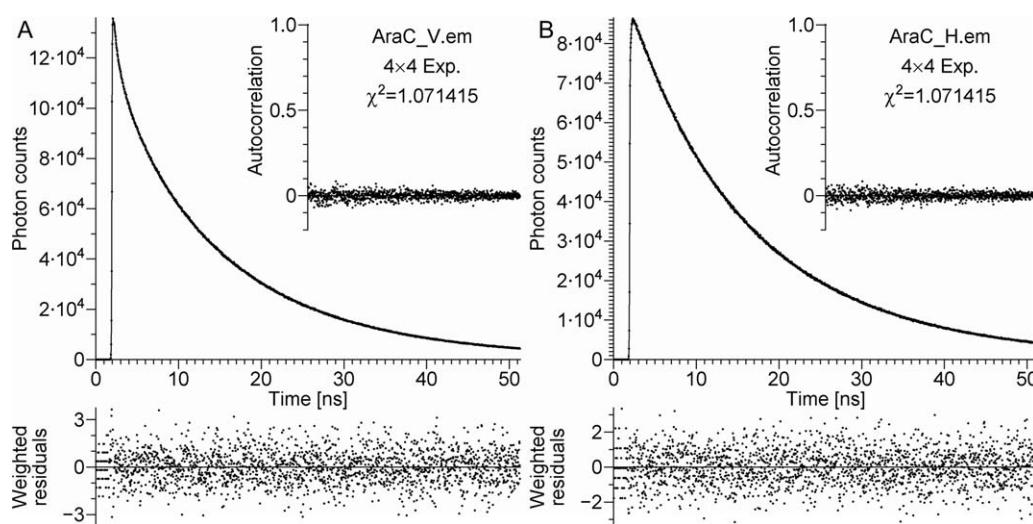

Figure 4

Time-resolved (**A**) vertically and (**B**) horizontally polarized data and fits to the data using four exponentials each for polarization and intensity obtained from 10 µM IAEDANS-labeled dimerization domain, 1.6 mL. By trial and error it was found that for adequate fit to the experimental data, the model must include $N_{ani} = 4$ exponentials for anisotropy decay and $N_{int} = 4$ exponentials for total intensity. The quality of the fits was judged using the values of the reduced χ^2 (must be under 1.08)[31] and also by inspecting the plots of weighted residuals and autocorrelations of residuals for each polarization separately.

Table II
Parameter Values with Standard Deviations for the Best Fits to the Data

Ligand		Exponential term index i			
		1	2	3	4
− Arabinose	φ_i (s)	0.147 ± 0.021	0.578 ± 0.066	4.44 ± 0.42	44.0 ± 1.0
	β_i	0.0561 ± 0.0042	0.0664 ± 0.0037	0.0330 ± 0.0018	0.0819 ± 0.0011
	τ_i (s)	0.213 ± 0.028	1.821 ± 0.097	10.37 ± 0.22	18.87 ± 0.21
	α_i	0.0858 ± 0.0024	0.0589 ± 0.0016	0.386 ± 0.019	0.469 ± 0.020
+ Arabinose	φ_i (s)	0.135 ± 0.022	0.637 ± 0.049	3.97 ± 0.26	40.63 ± 0.89
	β_i	0.0524 ± 0.0045	0.0738 ± 0.0044	0.0398 ± 0.0015	0.0699 ± 0.0009
	τ_i (s)	0.131 ± 0.015	1.396 ± 0.047	9.47 ± 0.16	16.90 ± 0.11
	α_i	0.110 ± 0.003	0.068 ± 0.001	0.312 ± 0.014	0.510 ± 0.014

intensity-weighted lifetimes of 16.1 ± 0.022 and 14.9 ± 0.011 ns, showing that the arabinose-induced reduction in anisotropy seen in the steady-state measurements is entirely due to an arabinose-induced increase in tumbling. Calculation of the steady-state anisotropies from the parameters in Table II yield 0.0719 ± 0.00037 and 0.0643 ± 0.00036 in the absence and presence of arabinose. These values are slightly different than those obtained on the steady-state instrument, which is probably due to the difference between the exciting wavelengths (311 nm in time-resolved vs. 336 nm in steady-state measurements). Nevertheless, the decrease in the anisotropy upon arabinose binding (0.0077 ± 0.0005) is in good agreement between both methods. Similar time-resolved measurements with IAEDANS labeling E63C, data not shown, showed that the overall tumbling rate of the dimerization domain is not increased by arabinose.

Arabinose binding to one subunit signals to only that linker on the other subunit

In the three-dimensional structure of the dimerization domain, the arabinose binding pocket of one subunit and the N-terminal arm that closes over the arabinose are significantly closer to the inter-domain linker of the other subunit than to the linker of the same subunit. We, therefore, tested the following possibilities: whether the binding of arabinose to one subunit affects the linker only of the opposite subunit, a *trans* effect; whether it affects the linker only of the same subunit, a *cis* effect; whether it affects the linkers on both subunits; or whether both subunits must bind arabinose in order that any signal be transmitted. The principle of the tests is diagrammed in Figure 5.

The anisotropy of linker-labeled H80A dimerization domain, which is unable to bind arabinose, should show no change upon arabinose addition. To this solution can then be added a large excess of unlabeled dimerization domain that is capable of binding arabinose. As subunit exchange proceeds, an increasing fraction, and eventually virtually all the arabinose-unresponsive IAEDANS-labeled subunits will be found in heterodimers with the unlabeled wild type subunits. If these heterodimers display

an arabinose response as shown by a decrease in anisotropy, two conclusions can be drawn. First, that the protein can respond to arabinose even if only one of its subunits has bound arabinose, and second, that a signal can be sent from the arabinose binding pocket of one subunit to the linker of the other subunit, a *trans* signal.

The second experiment diagrammed in Figure 5 is designed to test whether any signal is transmitted *cis*. The anisotropy of labeled dimer that is capable of binding arabinose will decrease upon arabinose addition. To this is added a large excess of unlabeled dimer that is incapable of binding arabinose. If, upon completion of subunit exchange, the arabinose response has been negated, then no signal is being sent *cis* and all the signal to a linker must derive from the *trans* subunit.

Figure 6 shows the experimental data from the two protocols described in Figure 5. The data displayed in panel A show that, IAEDANS-labeled dimerization domain that is incapable of binding arabinose displays no response to arabinose (inset) until an excess of
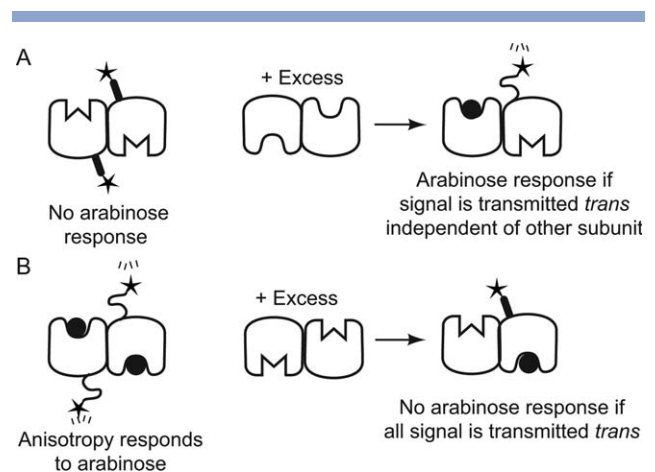

Figure 5

Schematic of heterodimer subunit exchange experiments to determine whether the signal from an arabinose binding pocket is transmitted to the *trans* or the *cis* linker, or to both. Sufficient excess of the nonlabeled dimerization domain must be added that at equilibrium the amount of labeled homodimer is negligible.
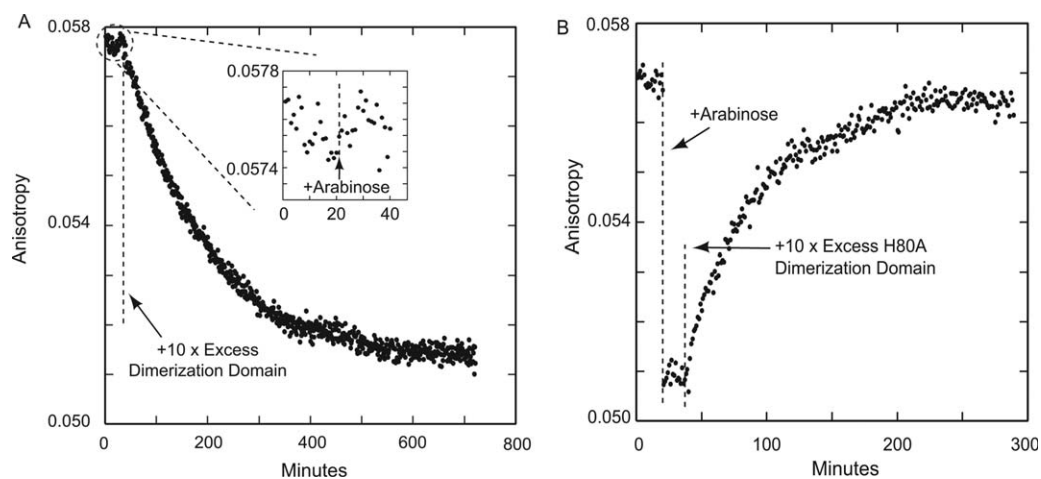
Figure 6

(**A**) Arabinose, to a concentration of 40 mM was added at 21 min to 0.48 μM H80A, incapable of binding arabinose, M175C-IAEDANS dimerization domain. At 40 min, a ×10 molar excess of unlabeled Y31V dimerization domain was added. (**B**) Arabinose, to a concentration of 40 mM was added at 20 min to 0.53 μM M175C-IAEDANS dimerization domain. At 40 min, a ×10 molar excess of unlabeled H80A dimerization domain was added.

unlabeled subunit capable of binding arabinose is added. This, together with the data shown in panel B show that all the signal for decreasing anisotropy is transmitted from the *trans* subunit, none is transmitted from the *cis* subunit, and that signal transmission is independent of the arabinose binding status of the other subunit. This experiment also provides the half-time of subunit exchange, which under these conditions, is seen to be about 60 min, similar to that measured for a mutant of full length AraC.[5]

DISCUSSION

In the genetics experiments reported here we find that normal functioning of AraC protein is possible despite substantial change in the sequence of its interdomain linker–as long as a proline residue is not substituted. When a proline reside is substituted for one of the first six linker residues, the protein becomes less capable of repressing. As proline is a strong helix breaker, this data hint that reduction of repression ability results from a reduction in the helical propensity of the linker region. It is, however, possible that the introduction of a proline residue destabilizes some other relatively rigid structure. Two additional factors are also suggestive of a helical linker. Immediately preceding the linker is an α-helix by which the protein dimerizes, and thus a helical state of the linker merely would extend the dimerization helix from 20 to as many as 26 residues. Second, in the crystal structures of apo dimerization domain, 1XJA, this helix extends an average of three residues further than in the crystal structures of the arabinose-bound dimerization domain, 2ARC.[6,21]

A shift in the interdomain linker of AraC from a stiff to a flexible state, whether or not it is a result of a helix-coil transition, could enable the protein to shift from forming a DNA loop by binding to the well separated *ara* I_1 and O_2 DNA half sites in the absence of arabinose to binding to the adjacent I_1 and I_2 half sites and inducing transcription in the presence of arabinose. To examine arabinose-induced tumbling or environmental changes at the end of the interdomain linker, we conjugated the fluorescent molecule IAEDANS to the end of the linker and monitored fluorescence anisotropy changes. We observed with AraC protein deleted of the DNA binding domain and consisting of dimerization domain plus linker that the fluorescence anisotropy decreases upon the addition of arabinose. Because time-resolved measurements showed that the excited-state lifetime of the IAEDANS had not been lengthened, but in fact, had been slightly shortened, the anisotropy decrease results from increased tumbling of the fluorophore. The tumbling mode with the shortest time constant, (Table II) most likely represents motion of the fluorophore independent of the linker arm to which it is attached. As its amplitude is not increased by arabinose addition, we suggest that the arabinose-induced decrease in anisotropy results from an increase in the flexibility of the linker. We emphasize, however, that the experimental data are changes in anisotropy, and that while plausible, changes in the flexibility of the linker have not rigorously been demonstrated by these experiments.

Further experiments utilizing fluorescent-labeled and unlabeled dimerization domain capable and incapable of binding arabinose, showed that the binding of arabinose to one subunit alters the anisotropy of a fluorophore on

only the other subunit. This is plausible physically because the arabinose binding pocket and N-terminal arm of one subunit are physically adjacent to the linker of the other subunit. We call this a *trans* regulation. Its existence indicates that a specific communication pathway exists between an arabinose binding pocket and the *trans* linker. This is in contrast to a global communication mechanism in which the binding of one arabinose molecule affects both subunits of the dimerization domain as a whole, and hence affects both linkers. The binding of one molecule of arabinose affecting the properties of only one linker would be consistent with two previously determined properties of AraC. First, that there is no detectable cooperativity or anti-cooperativity in the binding of arabinose to full length AraC or the dimerization domain,[21] and second, that the energetic effect on DNA binding of the binding of the first arabinose molecule is equal to the energetic effect of the second molecule.[5,21]

A number of control experiments support the basic findings. The fluorescence anisotropy of labeled linker is decreased by the arabinose, which binds to the dimerization domain of AraC, but not by other sugars that do not bind. The anisotropy change is a result of increased tumbling, and is not a result of a longer fluorescence lifetime of the IAEDANS. The fluorescence anisotropy of IAEDANS conjugated to a cysteine substitution at position 63 in the core of dimerization domain is not decreased by the binding of arabinose. Finally, the anisotropy of the linker-labeled dimerization domain does not show an arabinose response if the arabinose binding pocket of the protein has been mutated so that the protein does not bind arabinose.

It is unlikely that arabinose-dependent adventitious interactions between the conjugated IAEDANS and some part of the protein generated anomalous results. An interaction that altered the allosteric response of the protein would, of thermodynamic necessity,[57] have altered the affinity of arabinose binding. Conjugated IAEDANS, however, did not detectably alter the affinity of arabinose binding. Also, as noted earlier, the dynamics, as reflected in the amplitudes of the extracted anisotropy decay modes, do not support this interpretation.

While anisotropy studies on full-length AraC are of considerable interest, attempting such measurements is not sensible at present for several reasons. First, as mentioned in the introduction, AraC is of limited solubility and many mutants cannot be purified at all. Second, changes in the tumbling frequency of the DNA binding domain would be expected to be much less than changes in the tumbling frequency at the end of the interdomain linker without an attached DNA binding domain. Third, in the DNA-bound, plus arabinose state, the DNA binding domains cannot be symmetrically disposed, and hence two additional sets of tumbling modes are likely to be present.

A variety of previously published experiments have led to the suggestion that in the absence of arabinose, the DNA binding domains of AraC are held in orientations that restrict the protein's ability to bind to direct repeat DNA half-sites, that in the presence of arabinose, this restriction is reduced, and the protein can then bind tightly both the direct and inverted repeat DNA half-sites.[14,18] Despite much study, precisely how the change in DNA binding domain "adaptability" is generated has not been ascertained. The linker experiments described here are consistent with the idea that at least part of the arabinose-induced transition in AraC may lie in the inter-domain linker itself and that control of the positioning of the DNA binding domains is exerted on the linkers themselves and does not depend on the presence of the DNA binding domains. Although the N-terminal arm of AraC is involved, how it participates in this transition is not yet determined.

Ligand-responsive DNA binding proteins like transcription factors face a challenging problem generated by the fact that specificity for binding of the regulatory ligand normally resides in a domain separate from that responsible for binding to a specific sequence of DNA. How then can information about the status of the ligand binding site be transmitted to a DNA binding domain(s) to change the DNA binding affinity of the protein? In the three proteins that have been studied most extensively, AraC, LacI, and CAP, DNA binding affinity has been found to be modulated by controlling the relative positions and/or orientations of the DNA binding domains.[57,58] In the cases of LacI and CAP, the binding or release of a small molecule ligand controls a helix-coil transition of a portion of the protein,[38–41] and it is the rigidity-flexibility or structural integrity of this portion of the protein that plays a major role in controlling the positioning of the protein's DNA binding domains. Helix-coil transitions also appear to play a role in controlling the binding of TetR, the *tet* repressor.[5,21,42–44] Thus, the suggestion that arabinose controls the apparent flexibility of the inter-domain linker of AraC, and may do so via a helix-coil transition has precedence.

The involvement of inter-domain linkers in interactions relevant to activity has been examined in a number of other proteins. In IF3,[45] CytR,[46,47] RhaR, and RhaS,[48] existing data suggest that the inter-domain linker functions merely as a connector. It should be noted, however, that in these proteins extensive genetic and physical experiments have not yet been performed, and it is possible, just as it was in the case of AraC, that deeper analysis will reveal the existence of critical interactions between the linker and the rest of the protein. For still other proteins, Oct4,[49] DnaK,[50] and Hsp70[51] evidence has been found indicating that the linker interacts with something else, either a domain of the protein, or another protein. Finally, for a number of proteins XylR,[52] glucose transporter,[53] H-NS,[54] OmpR and

PhoB,[55] and CheA,[56] alterations in the linker have been found that appreciably alter the activity of the protein by altering domain-domain interactions.

In summary, the functioning of AraC appears to be largely unaffected by many mutations in the interdomain linker—unless the mutation inserts a proline residue. In these cases, the ability of AraC to repress activity of p_{BAD} is impaired. Fluorescence anisotropy experiments on dimerization domain plus linker with IAEDANS conjugated to the end of the linker show that the binding of arabinose to one dimerization domain specifically increases the tumbling of the fluorophore on the other dimerization domain. It is possible that the increased tumbling seen in the various experiments presented in this article represents increased flexibility in the linker, which possibly could result from decreased propensity of the linker to be in a helical state. However, such a conjecture remains to be proven.

REFERENCES

1. Schleif R. AraC protein, regulation of the L-arabinose operon in Escherichia coli, and the light switch mechanism of AraC action. FEMS Microbiol Rev 2010;34:779–796.
2. Li Z, Demple B. SoxS, an activator of superoxide stress genes in Escherichia coli. Purification and interaction with DNA. J Biol Chem 1994;269:18371–18377.
3. Rhee S, Martin RG, Rosner JL, Davies DR. A novel DNA-binding motif in MarA: the first structure for an AraC family transcriptional activator. Proc Natl Acad Sci USA 1998;95:10413–10418.
4. Lowden MJ, Skorupski K, Pellegrini M, Chiorazzo MG, Taylor RK, Kull FJ. Structure of Vibrio cholerae ToxT reveals a mechanism for fatty acid regulation of virulence genes. Proc Natl Acad Sci USA 2010;107:2860–2865.
5. Rodgers ME, Schleif R. Heterodimers reveal that two arabinose molecules are required for the normal arabinose response of AraC. Biochemistry (NY) 2012;51:8085–8091.
6. Soisson SM, MacDougall-Shackleton B, Schleif R, Wolberger C. Structural basis for ligand-regulated oligomerization of AraC. Science 1997;276:421–425.
7. Timmes A, Rodgers M, Schleif R. Biochemical and physiological properties of the DNA binding domain of AraC protein. J Mol Biol 2004;340:731–738.
8. Englesberg E, Irr J, Power J, Lee N. Positive control of enzyme synthesis by gene C in the L-arabinose system. J Bacteriol 1965;90:946–957.
9. Englesberg E, Squires C, Meronk FJ. L-Arabinose operon in Escherichia coli B/r; genetic demonstration of two functional states of the product of a regulator gene. Proc Natl Acad Sci USA 1969;62:1100–1107.
10. Martin K, Huo L, Schleif RF. The DNA loop model for ara repression: AraC protein occupies the proposed loop sites in vivo and repression-negative mutations lie in these same sites. Proc Natl Acad Sci USA 1986;83:3654–3658.
11. Dunn TM, Hahn S, Ogden S, Schleif RF. An operator at -280 base pairs that is required for repression of araBAD operon promoter: addition of DNA helical turns between the operator and promoter cyclically hinders repression. Proc Natl Acad Sci USA 1984;81:5017–5020.
12. Lee DH, Schleif RF. In vivo DNA loops in araCBAD: size limits and helical repeat. Proc Natl Acad Sci USA 1989;86:476–480.
13. Lobell RB, Schleif RF. DNA looping and unlooping by AraC protein. Science 1990;250:528–532.
14. Seabold RR, Schleif RF. Apo-AraC actively seeks to loop. J Mol Biol 1998;278:529–538.
15. Irr J, Englesberg E. Control of expression of the L-arabinose operon in temperature-sensitive mutants of gene araC in Escherichia coli B/r. J Bacteriol 1971;105:136–141.
16. Greenblatt J, Schleif R. Arabinose C protein: regulation of the arabinose operon in vitro. Nat New Biol 1971;233:166–170.
17. Hirsh J, Schleif R. The araC promoter: transcription, mapping and interaction with the araBAD promoter. Cell 1977;11:545–550.
18. Carra JH, Schleif RF. Variation of half-site organization and DNA looping by AraC protein. EMBO J 1993;12:35–44.
19. Saviola B, Seabold R, Schleif RF. Arm-domain interactions in AraC. J Mol Biol 1998;278:539–548.
20. Ross JJ, Gryczynski U, Schleif R. Mutational analysis of residue roles in AraC function. J Mol Biol 2003;328:85–93.
21. Weldon JE, Rodgers ME, Larkin C, Schleif RF. Structure and properties of a truely apo form of AraC dimerization domain. Proteins 2007;66:646–654.
22. Dirla S, Chien JY, Schleif R. Constitutive mutations in the Escherichia coli AraC protein. J Bacteriol 2009;191:2668–2674.
23. Wu M, Schleif R. Mapping arm-DNA-binding domain interactions in AraC. J Mol Biol 2001;307:1001–1009.
24. Ghosh M, Schleif RF. Biophysical evidence of arm-domain interactions in AraC. Anal Biochem 2001;295:107–112.
25. Rodgers ME, Holder ND, Dirla S, Schleif R. Functional modes of the regulatory arm of AraC. Proteins 2009;74:81–91.
26. Eustance RJ, Schleif RF. The linker region of AraC protein. J Bacteriol 1996;178:7025–7030.
27. Seedorff J, Schleif R. Active role of the interdomain linker of AraC. J Bacteriol 2011;193:5737–5746.
28. Balbás P, Soberón X, Merino E, Zurita M, Lomeli H, Valle F, Flores N, Bolivar F. Plasmid vector pBR322 and its special-purpose derivatives - a review. Gene 1986;50:3–40.
29. Hahn S, Dunn T, Schleif R. Upstream repression and CRP stimulation of the Escherichia coli L-arabinose operon. J Mol Biol 1984;180:61–72.
30. Schleif RF, Wensink PC. Practical methods in molecular biology. New York: Springer-Verlag; 1981. 220 p.
31. Toptygin D. Analysis of time-dependent red shifts in fluorescence emission from tryptophan residues in proteins. In: Engelborghs Y, Visser AJWG, editors. Fluorescence spectroscopy and microscopy: methods and protocols. Totowa, NJ: Humana Press; 2014. pp 215–256.
32. Lakowicz JR. Principles of fluorescence spectroscopy. USA: Springer-Verlag; 2006.
33. Toptygin D, Savtchenko RS, Meadow ND, Brand L. Homogeneous spectrally- and time-resolved fluorescence emission from single-tryptophan mutants of IIAGlc protein. J Phys Chem B 2001;105:2043–2055.
34. Chen J, Toptygin D, Brand L, King J. Mechanism of the efficient tryptophan fluorescence quenching in Human gammaD-crystallin studied by time-resolved fluorescence. Biochemistry (NY) 2008;47:10705–10721.
35. Pierce BD, Toptygin D, Wendland B. Pan1 is an intrinsically disordered protein with homotypic interactions. Proteins 2013;81:1944–1963.
36. Hamilton WC. Statistics in physical sciences: estimation, hypothesis testing, and least squares. New York: Ronald Press; 1964.
37. Cole SD, Schleif R. A new and unexpected domain-domain interaction in the AraC protein. Proteins 2012;80:1465–1475.
38. Sharma H, Yu S, Kong J, Wang J, Steitz TA. Structure of apo-CAP reveals that large conformational changes are necessary for DNA binding. Proc Natl Acad Sci USA 2009;106:16604–16609.
39. Popovych N, Tzeng S, Tonelli M, Ebright RH, Kalodimos CG. Structural basis for cAMP-mediated allosteric control of the catabolite activator protein. Proc Natl Acad Sci USA 2009;106:6927–6932.S6927/1-S6927/12.

40. Bell CE, Lewis M. A closer view of the conformation of the Lac repressor bound to operator. Nat Struct Mol Biol 2000;7:209–214.

41. Bell CE, Lewis M. The Lac repressor: a second generation of structural and functional studies. Curr Opin Struct Biol 2001;11:19–25.

42. Orth P, Cordes F, Schanppinger D, Hillen W, Saenger W, Hinrichs W. Conformational changes in the Tet repressor induced by tetracycline trapping. J Mol Biol 1998;279:439–447.

43. Orth P, Schnappinger D, Hillen W, Saenger W, Hinrichs W. Structural basis of gene regulation by the tetracycline inducible Tet repressor-operator system. Nat Struct Biol 2000;7:215–219.

44. HinrichsW, Kisker C, Duvel M, Muller A, Tovar K, Hillen W, Saenger W. Structure of the Tet repressor-tetracycline complex and regulation of antibiotic resistance. Science 1994;264:418–420.

45. de Cock E, Springer M, Dardel F. The interdomain linker of Escherichia coli initiation factor IF3: a possible trigger of translation initiation specificity. Mol Microbiol 1999;32:193–202.

46. Jørgensen CI, Kallipolitis BH, Valentin-Hansen P. DNA-binding characteristics of the Escherichia coli CytR regulator: a relaxed spacing requirement between operator half-sites is provided by a flexible, unstructured interdomain linker. Mol Microbiol 1998;27:41–50.

47. Kallipolitis BH, Valentin-Hansen P. A role for the interdomain linker region of the Escherichia coli CytR regulator in repression complex formation. J Mol Biol 2004;342:1–7.

48. Kolin A, Jevtic V, Swint-Kruse L, Egan SM. Linker regions of the RhaS and RhaR proteins. J Bacteriol 2007;189:269–271.

49. Esch D, Vahokoski J, Groves MR, Pogenberg V, Cojocaru V, vom Bruch H, Han D, Drexler HCA, Araúzo-Bravo MJ, Ng CKL, Jauch R, Wilmanns M, Schöler HR. A unique Oct4 interface is crucial for reprogramming to pluripotency. Nat Cell Biol 2013;15:295–301.

50. Han W, Christen P. Mutations in the interdomain linker region of DnaK abolish the chaperone action of the DnaK/DnaJ/GrpE system. FEBS Lett 2001;497:55–58.

51. Kumar DP, Vorvis C, Sarbeng EB, Cabra L, Vanessa C, Willis JE, Liu Q. The four hydrophobic residues on the Hsp70 interdomain linker have two distinct roles. J Mol Biol 2011;411:1099–1113.

52. Garmendia J, de Lorenzo V. The role of the interdomain B linker in the activation of the XyIR protein of Pseudomonas putida. Mol Microbiol 2000;38:401–410.

53. Lanz R, Erni B. The glucose transporter of the Escherichia coli phosphotransferase system. Mutant analysis of the invariant arginines, histidines, and domain linker. J Biol Chem 1998;273:12239–12243.

54. Mellies JL, Larabee FJ, Zarr MA, Horback KL, Lorenzen E, Mavor D. Ler interdomain linker is essential for anti-silencing activity in enteropathogenic *Escherichia coli*. Microbiology (Reading, U K) 2008;154:3624–3638.

55. Walthers D, Tran VK, Kenney LJ. Interdomain linkers of homologous response regulators determine their mechanism of action. J Bacteriol 2003;185:317–324.

56. Wang X, Wu C, Vu A, Shea J, Dahlquist FW. Computational and experimental analyses reveal the essential roles of interdomain linkers in the biological function of chemotaxis histidine kinase CheA. J Am Chem Soc 2012;134:16107–16110.

57. Schleif RF. Modulation of DNA binding by gene-specific transcription factors. Biochemistry (NY) 2013;52:6755–6765.

58. Seedorff JE, Rodgers ME, Schleif R. Opposite allosteric mechanisms in TetR and CAP. Protein Sci 2009;18:775–781.